Determination of the Filler Distribution in an Epoxy Molding Compound Using High-Resolution X-ray Computed Tomography

E. Topal*, J. Gluch, A. Clausner, A. Cardoso, E. Zschech

Abstract—**In this paper, the filler distribution in an epoxy molding compound (EMC), used in IC packaging, is studied across a wafer using high-resolution X-ray computed tomography (HR-XCT). It is widely assumed that the fillers are uniformly distributed across the wafer. However, it is demonstrated that the distribution of the filler deviates across the wafer, and that filler sizes affect the distribution on edge and center of wafer too. Quantitative HR-XCT of the filler distribution provides accurate data for simulation. Based on this approach, the differences between CTE and Young's modulus values of the filler material for the center and edge of the wafer is explained. Furthermore, compression simulations are conducted applying an XCT-based FEM model to understand the role of EMC for the mechanical behavior of advanced IC packages. These findings are validated by in-situ and stand-alone compression experiments. The accurate simulation results demonstrate that the use of an XCT-based FEM model provides insight into the mechanical behavior of the EMC itself, and furthermore, of the whole IC package.**

Index Terms—**Computed tomography, Finite element analysis, Semiconductor device packaging**

I. Introduction

EPOXY molding compounds (EMCs) are widely used for encapsulation of microelectronic products to protect them from physical or chemical environmental effects such as temperature, moisture, chemical agents, dust and stress [1], [2]. Semiconductor industry is intensifying its efforts to functionalize the package because of an increasing demand for highly integrated high-performance microelectronic products with low power consumption [3], [4]. This trend includes particularly 2.5D and 3D advanced packaging [5]–[7]. As one of these new approaches, fan-out wafer level packaging (FO-WLP) is a fast-growing advanced packaging technology mainly due to its low cost, good electrical and thermal performance, low profile package and easy-to-go for system-in-package (SiP) and 3D IC packaging [6], [8]. A typical FO-WLP process requires a reconstituted carrier for the known-good die (KGD), EMC, compression molding, and the fabrication of the redistribution layers (RDLs). The EMC is one of the main elements of FO-WLPs and it plays a critical role for a stable chip performance. The EMC is a polymer matrix composite that usually contains many components, such as organic resins, micro-sized non-melting inorganic fillers, adhesion promoters, ion traps and stress relievers. However, among these materials, micro sized fillers made of amorphous SiO_2 are a major fraction of the volume. The role of these fillers is to strengthen the epoxy resin and to increase the Young's modulus of the EMC [9], [10]. Thus, size and distribution of these fillers in the EMC affect the mechanical properties of the EMC [11]. It was shown that a smaller filler size might improve the reliability of the package [12]. Wafer warpage after molding and EMC curing is a result of mismatched coefficients of thermal expansion (CTE) and of shrinkage caused by curing. Previous studies showed that a higher filler quantity results in a lower CTE of the EMC and in a decrease of the chemical cure shrinkage [13]. Both effects reduce the warpage.

The FEM simulation is a commonly used approach to understand the dynamic warpage behavior of the package, particularly to accurately predict the package warpage and to refine the process and design parameters [12]. Therefore, it is critical to consider the process-dependent constitutive behaviors of the packaging materials. An inhomogeneous filler distribution across the wafer can significantly affect the wafer warpage, which can have a significant impact on processability. So far, all experimental studies, simulations and considerations assume that the EMC is uniformly distributed across the wafer. A systematic characterization of the filler distribution would provide important input for simulation, and moreover, it would help to explain the differences of CTE and Young's modulus values between the center and edge of the wafer. Since the filler significantly affects the mechanical properties of the EMC, it is especially important to characterize the filler distribution quantitatively. Therefore, the focus of this paper is on analyzing the variation of the filler distribution in EMC across the wafer.,

Submitted for review on 01.03.2020.

This work was supported financially supported by the European Commission as a part of ECSEL joint undertaking project "EuroPAT-MASIP".

E. Topal was with the Technische Universität Dresden, Dresden Center for Nanoanalysis, 01062 Dresden, Germany (e-mail: emre.topal@tu-dresden.de). E. Zschech is with the Fraunhofer Institute for Ceramic Technologies and Systems Dresden as well as with Technische Universität Dresden, and Dresden Center for Nanoanalysis, 01109 Dresden, Germany (e-mail: ehrenfried.zschech@ikts.fraunhofer.de). J. Gluch and A. Clausner are with the Fraunhofer Institute for Ceramic Technologies and Systems Dresden, 01109 Dresden, Germany (e-mail: juergen.gluch@ikts.fraunhofer.de, andre.clausner@ikts.fraunhofer.de). A. Cardoso is with Amkor Technologies Portugal, Vila do Conde, Portugal (e-mail: andre.cardoso@amkor.com).

Accurate 3D images of the filler material, based on laboratory nano-XCT studies, are used as input for the calculation of the filler distribution in EMCs. Furthermore, the measured 3D volume is used to develop a FEM model for the investigation of the mechanical behavior of the EMC, which considers the real filler shape, size and distribution. The compression experiments are conducted to acquire load-displacement curves for validation of the FEM simulations. Finally, the simulation results are validated with the data from in-situ nano-XCT experiments.

II. Materials and Experimental Setup

A. Sample Preparation

Two wafers with two different, commercially available EMC types with identical resin but different filler sizes and filler size distributions, named as EMC1 and EMC2, were processed using the FO-WLP technology [14] at identical process parameters. After the compress molding process, both wafers were cured, initially at 150°C and subsequently at 200°C.

After wafer dicing, separated dies were picked up from the wafer. Afterwards, the samples with 4 dies were sawed using a wafer saw. In order to investigate the EMC samples using laboratory nano-XCT at a photon energy of 8 keV, the samples were flipped and thinned down from the backside to 50 µm. Ultimately, cuboids with a size of 50x60x90 μm^3 were picked up from the die and mounted on a sample holder. The scheme that visualizes the sample preparation steps is given in Fig. 1.

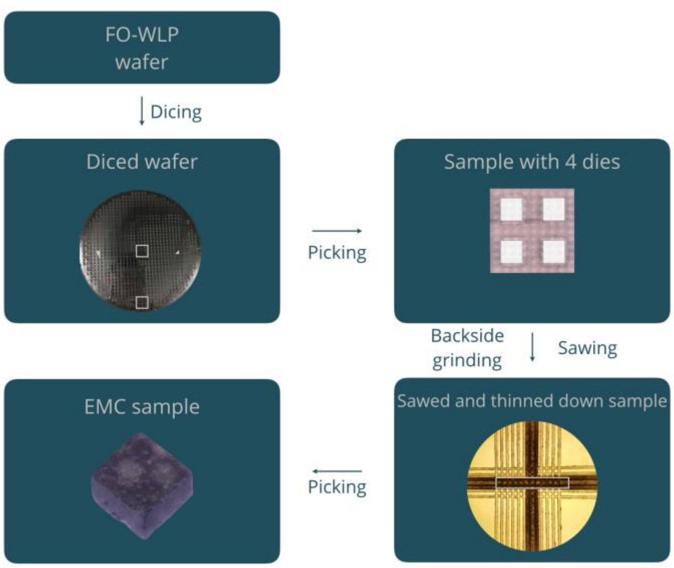

Fig. 1. The workflow used for preparation of the samples for nano-XCT studies. The marked regions show the locations samples are picked from.

In order to investigate the filler distribution in EMC across the wafer, cuboid samples were selected from the scribeline at the center and at the edge of the wafers. These samples were named as EMC1/2-C and EMC1/2-E, respectively.

B. Structural Characterization and Nano X-ray Computed Tomography Data Acquisition and Reconstruction

The laboratory nano-XCT tool (Xradia Ultra 100) was used in high-resolution mode at a photon energy of 8 keV. The field of view was 66.5x66.5 μm^2 with 512x512 pixels, resulting in a voxel size of 0.13 µm. The tilt series for tomography consisted of 401 images covering an angular range of 180°. The exposure time per image was 210s and 180s for EMC1 and EMC2, respectively.

The acquired radiographs were reconstructed using an in-house developed reconstruction software based on the Filtered Back Projection (FBP) algorithm [15], [16]. This reconstruction methodology provides highly accurate 3D data of the microstructure of materials, considering corrections for imaging artefacts in high-resolution XCT caused by tool misalignments and motions of samples and tool components using AI algorithms [16], [17]. Eventually, the reconstructed images were segmented to visualize and to calculate the filler distribution of the EMC samples using the Avizo software [18].

C. Mechanical Characterization

A triboindenter tool (Hysitron TI 950) was used to investigate the mechanical behavior of EMC materials through stand-alone compression experiments. A diamond flat punch indenter with a cylindrical tip of 54 µm radius was used and a load of up to 1400 mN load was applied. The same experiment was replicated using an in-situ indenter setup that was integrated into the nano-XCT tool to observe in-situ compression experiments (see Fig. 2). The same tip was used and a load of up to 800 mN load was applied. This experimental setup enables to measure the local material response that is characteristic for the micromechanical behavior of the EMC. The radiographs were recorded during the compression experiment, and the load versus displacement data were extracted.

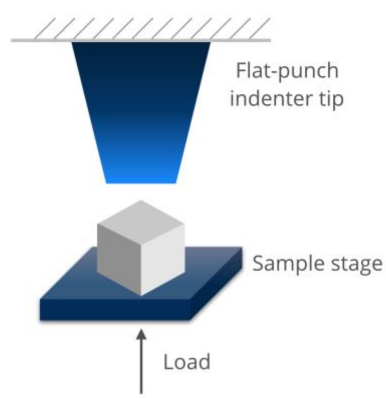

Fig. 2. The setup of in-situ compression experiment. The setup allows to record radiographs during the experiment.

D. *Finite Element Analysis*

The 3D reconstructed XCT data were used as input to create a "digital twin" of the mechanically investigated one. The workflow for the simulation of the EMCs is provided in Fig. 3. The reconstructed image stack was segmented and converted into a surface mesh using the Simpleware ScanIp software [19], which enables to preserve all features of the EMCs. Subsequently, a reverse engineering approach using Ansys SpaceClaim tools [20] was applied to generate the geometry of the EMC samples. This approach provides a high flexibility for building different models that might require different simulation setups. Finally, a tetrahedral mesh was generated using the finite-element software ANSYS [21], and a nonlinear geometry solver was implemented to capture large deflections of the structure. The final mesh consisted of 1.2m nodes and 7m elements with an average aspect ratio of 2.11 and an average mesh quality of 0.76. The compression tests are replicated in the FEM framework in order to understand the effect of the fillers on the mechanical behavior of the EMC. The load-displacement data obtained in the in-situ and stand-alone compression tests were used to validate the FEM simulations. The studied EMCs consisted of three components: SiO_2 filler, metal filler, and epoxy. The respective material models are given in Table 1.

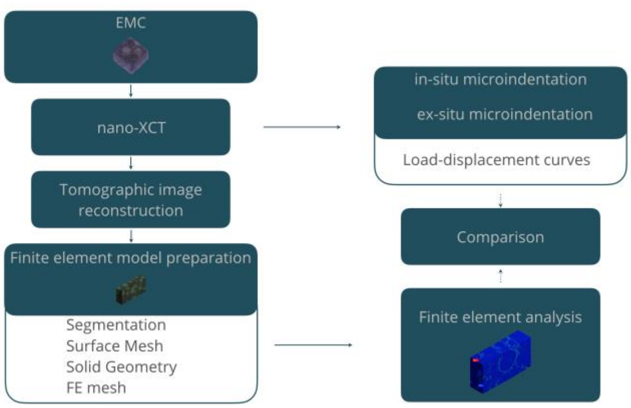

Fig. 3. The workflow used to create a FEM model of the mold compound

TABLE I
MATERIAL MODEL

Material Property	Metal Filler	Silica Filler	Epoxy
Young's Modulus (GPa)	110	73	3.7
Bulk Modulus (GPa)	110	35	4.2
Poisson's Ratio	0.34	0.155	0.35

III. RESULTS AND DISCUSSION

The virtual cross-sections from reconstructed nano-XCT data of the EMC1 and EMC2 samples are shown in Fig. 4 and Fig. 5, respectively. The SiO_2 filler, the metal filler, and the voids in the epoxy are visualized in 3D. The size of the reconstructed volume for each sample was about 64x65x66 μm^3.

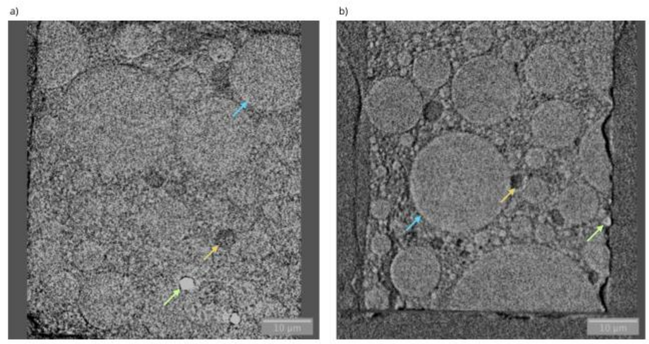

Fig. 4. Virtual cross-sections from reconstructed nano-XCT data of the EMC1 sample from a) the edge of the wafer and b) the center of the wafer. Blue arrow: SiO_2 filler, yellow arrow: void, and green arrow: metal filler.

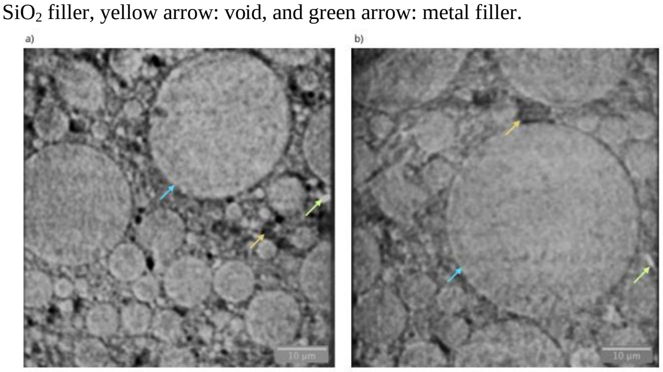

Fig. 5. Virtual cross-sections from reconstructed nano-XCT data of the EMC2 sample at a) the edge of the wafer and b) the center of the wafer. Blue arrow: SiO_2 filler, yellow arrow: void, and green arrow: metal filler.

A. *Filler Distribution in an Epoxy Molding Compound*

After the segmentation, the images were processed to identify and to label every individual SiO_2 sphere filler within the 3D volume, and thus, it was possible to quantify number, diameter and volume of these spheres. The labels were classified into groups according to their diameters, and they were visualized with different colors in Fig. 6.

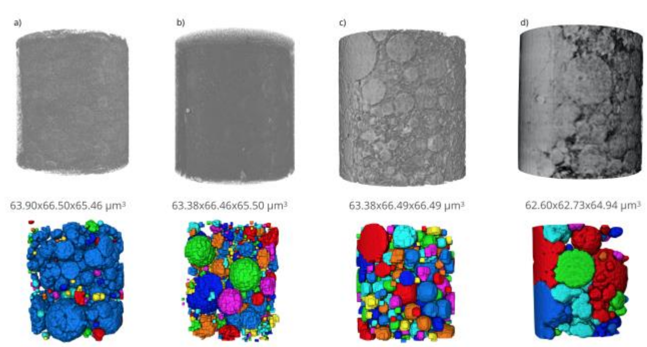

Fig. 6. The reconstructed volumes for all four samples and their respective classified filler diameter visualizations: a) EMC1E, b) EMC1C, c) EMC2E, and d) EMC2C

Ultimately, in order to compare the filler distribution across the wafer, histograms were used for EMC1 and EMC2, shown in Fig. 7 and 8, respectively, and summarized in Table 2.

TABLE I
FILLER DISTRIBUTION

	EMC1		EMC2	
Location	Edge	Center	Edge	Center
Detected number of spheres	149	401	277	154
Average diameter (µm)	29.3	28.5	6.3	7.7
10-20 µm (%)	34.2	50.6	Not relevant	Not relevant
20-30 µm (%)	19.0	39.6	Not relevant	Not relevant
0-4 µm (%)	Not relevant	Not relevant	28.9	8.4
4-8 µm (%)	Not relevant	Not relevant	48.0	57.8

For the EMC1E sample, 149 spheres were identified with an average diameter of 29.3 µm. 34.2% of these spheres have a diameter in the range of 10-20 µm and 19% in the range of 20-30 µm. For the EMC1C sample, 401 spheres were identified with an average diameter of 28.5 µm. 50.6% of these spheres have a diameter in the range of 10-20 µm and only 39.6% in the range of 20-30 µm. That means for the EMC1 sample that the EMC on the edge of the wafer has less filler compared to the EMC on the center of the wafer, and the majority of filler has slightly larger diameters.

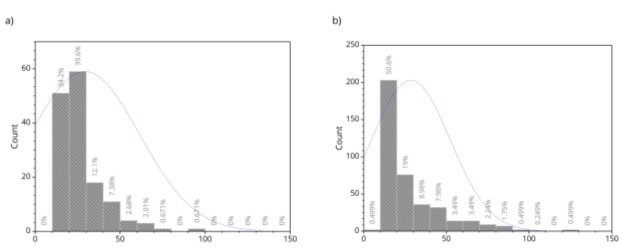

Fig. 7. The distribution of fillers within the investigated volumes of the EMC1 sample: from a) the edge of the wafer and b) the center of the wafer.

For the EMC2E sample, 277 spheres were identified with an average diameter of 6.3 µm. 48% of these spheres have a diameter in the range of 4-8 µm and 28.9% in the range of 0-4 µm. For the EMC2C sample, 154 spheres were identified with an average diameter of 7.7 µm. 57.8% of these spheres have a diameter in the range of 4-8 µm and only 8.4% in the range of 0-4 µm. That means for the EMC2 sample that the EMC at the edge of the wafer has more filler compared to the EMC at the center of wafer. This result is different to the observations for EMC1. That means, a smaller filler diameter - the average filler diameter of EMC2 was significantly smaller compared to EMC1 - reduces the deviation of filler distribution across the wafer.

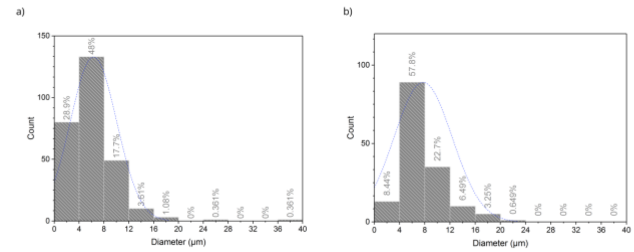

Fig. 8. The distribution of fillers within the investigated volumes of the EMC2 sample: at a) the edge of the wafer and b) the center of the wafer.

B. *Mechanical Characterization*

An in-situ compression test using a flat punch indenter in the nano-XCT tool [22] was performed for sample EMC2C to analyze the behavior of the fillers under the load. The in-situ experiment was conducted for continuous loading condition with small step sizes. At each load step, two radiographs were recorded with 120 seconds exposure time. This recording time served as holding time for each load step. The load was gradually increased up to 800 mN, and the displacements were calculated from the acquired radiographs. The respective load-displacement curve is shown in Fig. 9.

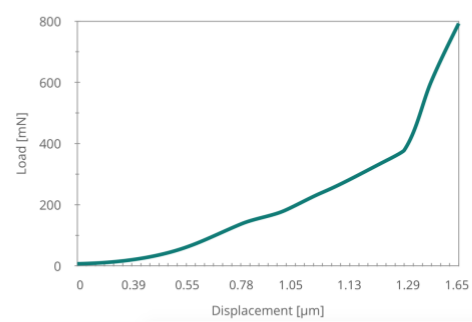

Fig. 9. The load-displacement curve obtained from in-situ experiments. The load is recorded through the in-situ tool and the displacements are calculated from acquired radiographs at each load step.

The observed crack propagation during loading is shown in Fig. 10. The cracks, initiated at the interface between epoxy and filler at a load of 400 mN, propagated along the interface with increasing load steps. At 600 mN, the crack became clearly visible, and it propagated at 800 mN to neighbored interface.

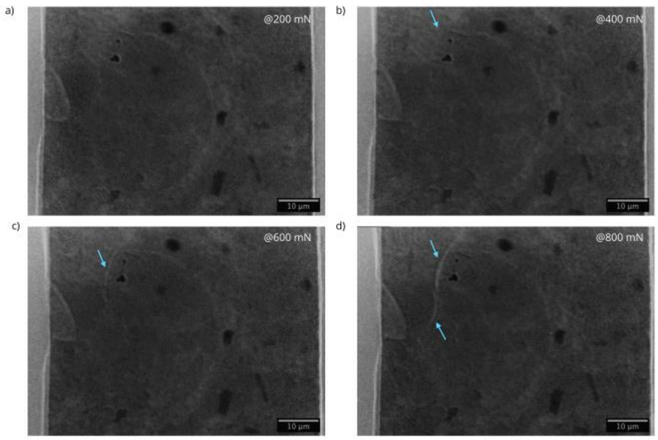

Fig. 10. The acquired radiographs during the in-situ compression experiment for a load of a) 200 mN, b) 400 mN, c) 600 mN and d) 800 mN. The arrows highlight the crack propagation.

After the in-situ compression test, the same sample was investigated through stand-alone experiments in order to compare the obtained displacement, which was calculated through recorded radiographs, and also to provide input for the FEM analysis. The load-displacement curves are shown in Fig. 11. The holding time for each loading step was 20s. These load-displacement curves confirmed that the EMC shows an elastic-plastic response under compression and a plastic deformation of 0.57 µm at a load of 800 mN. For a load of 1200 mN, the behavior was similar, however, the plastic deformation was 1.2 µm, with an obvious creep behavior.

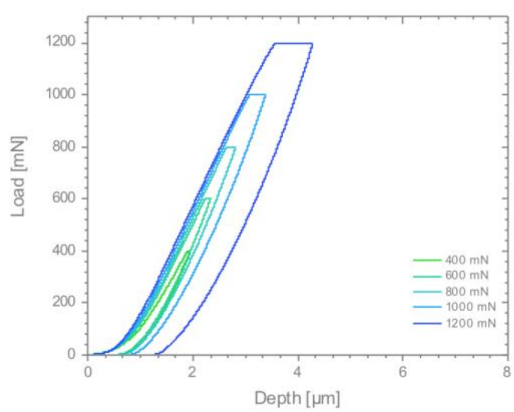

Fig. 11. The load-displacement curves for a load range between 400 mN and 1200 mN.

C. Finite Element Analysis

Finally, the reconstructed XCT data of sample EMC2C was used to construct a model, and the compression test was replicated within the FEM framework. The model and the boundary condition are given in Fig. 12.

The simulation of the compression test was conducted for 3 load steps: 400 mN, 600 mN and 800mN. The load-displacement values obtained from the simulation were compared and validated with the in-situ and stand-alone experiments, see Fig. 13.

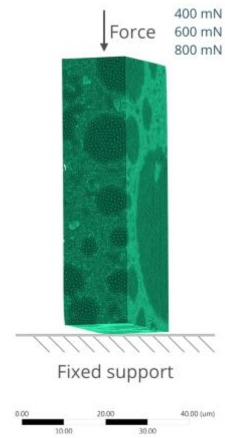

Fig. 12. The XCT-based FEM model of EMC2C. The load used to compress the EMC block from the top surface. A fixed support is applied to stabilize the model. The final mesh consists of 1.2m nodes and 7m elements with an average aspect ratio of 2.11 and an average mesh quality of 0.76.

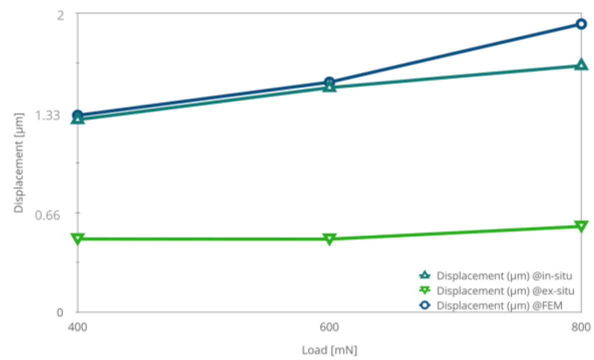

Fig. 13. The comparison of load-displacement values obtained from XCT-based-FEM compression simulation, in-situ compression test and stand-alone compression test.

The displacement values calculated from obtained radiographs were higher for the in-situ experiments compared to the stand-alone experiments. The difference can be explained by the longer holding time required for the acquisition of the radiographs of in-situ experiments in nano-XCT, compared to continuous loading for the stand-alone experiments. The displacements obtained from the simulation are close to the ones observed from the in-situ experiments, with a maximum deviation difference of 0.27 µm at 800 mN between experiments and simulations. This result proves the proposed approach to use XCT-based FEM. The achieved similar displacements allow to correlate the stress and strain fields with the observed crack propagation. Furthermore, the simulation results enable to calculate strain and stress fields together with deformation as shown in Fig. 14. As expected, the deformation field is dispersed by the fillers. In the in-situ compression experiment, the crack initiation is observed around the larger fillers. In the simulation, we observed a higher strain around the largest filler in our model. Therefore, we conclude that crack propagation can be explained with the high strain fields.

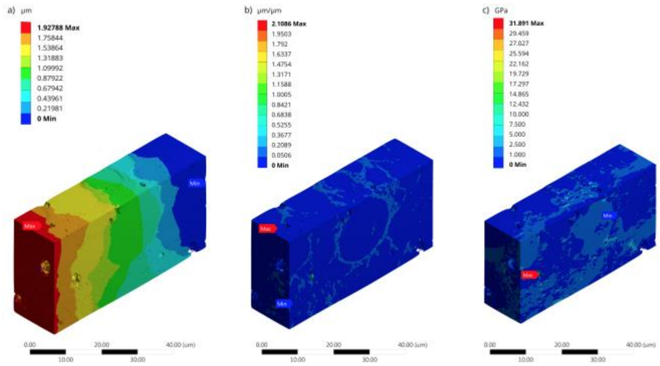

Fig. 14. The compression simulation results of XCT-based FEM model under at a load of 800 mN: a) total deformation, b) equivalent elastic strain, and c) equivalent stress

IV. Conclusions

Nano-XCT images of EMC samples were applied to visualize the filler size and the 3D filler distribution across the wafer quantitatively. The filler distribution across the wafer is affected by the filler size and it varies significantly from the wafer center to the wafer edge. Since these 3D microstructure data are directly correlated to CTE and Young's modulus values, which are different at the center and at the edge of the wafer too, the data can be used to validate and to improve modelling and simulation. Furthermore, the reconstructed 3D volume itself can be used to construct a FEM model identical to as-processed EMCs to obtain more realistic simulation results compared to simplified models. This is a solid precondition for the use of this approach for process control. Future work will be directed on thermo-mechanical simulation of EMCs for further understanding of the effect of the filler distribution on wafer warpage.

Acknowledgment

This work was supported by financing from European Commission as a part of ECSEL joint undertaking project "EuroPAT-MASIP".

References

[1] J. H. Lupinski and R. S. Moore, "Polymeric Materials for Electronics Packaging and Interconnection: An Overview," in *Polymeric Materials for Electronics Packaging and Interconnection*, vol. 407, J. H. Lupinski and R. S. Moore, Eds. Washington, DC: American Chemical Society, 1989, pp. 1–24.

[2] C. Xu, Z. W. Zhong, and W. K. Choi, "Epoxy molding compound effect on fan-out wafer level package strength during post-mold thermal process," in *2017 16th IEEE Intersociety Conference on Thermal and Thermomechanical Phenomena in Electronic Systems (ITherm)*, Orlando, FL, 2017, pp. 1388–1392, doi: 10.1109/ITHERM.2017.7992643.

[3] E. J. Vardaman, "FO-WLP Market and Technology Trends," in *Advances in Embedded and Fan-Out Wafer-Level Packaging Technologies*, B. Keser and S. Kroehnert, Eds. Hoboken, NJ, USA: John Wiley & Sons, Inc., 2019, pp. 39–54.

[4] D. Lu and C. P. Wong, Eds., *Materials for Advanced Packaging*. Boston, MA: Springer US, 2009.

[5] R. Huemoeller and C. Zwenger, "SWIFT® Semiconductor Packaging Technology," in *Advances in Embedded and Fan-Out Wafer-Level Packaging Technologies*, B. Keser and S. Kroehnert, Eds. Hoboken, NJ, USA: John Wiley & Sons, Inc., 2019, pp. 141–167.

[6] J. H. Lau, "Recent Advances and Trends in Fan-Out Wafer/Panel-Level Packaging," *Journal of Electronic Packaging*, vol. 141, no. 4, p. 040801, Dec. 2019, doi: 10.1115/1.4043341.

[7] T. G. Lim, D. S. W. Ho, E. W. L. Ching, Z. Chen, and S. Bhattacharya, "FOWLP Design for Digital and RF Circuits," in *2019 IEEE 69th Electronic Components and Technology Conference (ECTC)*, Las Vegas, NV, USA, 2019, pp. 917–923, doi: 10.1109/ECTC.2019.00143.

[8] J. H. Lau, *3D IC integration and packaging*. New York: McGraw-Hill Education, 2016.

[9] M. Linec and B. Mušič, "The Effects of Silica-Based Fillers on the Properties of Epoxy Molding Compounds," *Materials*, vol. 12, no. 11, p. 1811, Jun. 2019, doi: 10.3390/ma12111811.

[10] J. K. W. Sandler, J. E. Kirk, I. A. Kinloch, M. S. P. Shaffer, and A. H. Windle, "Ultra-low electrical percolation threshold in carbon-nanotube-epoxy composites," *Polymer*, vol. 44, no. 19, pp. 5893–5899, Sep. 2003, doi: 10.1016/S0032-3861(03)00539-1.

[11] Yue Huang, D. Bigio, and M. G. Pecht, "Investigation of the size and spatial distribution of fillers in mold compounds after device packaging," *IEEE Trans. Comp. Packag. Technol.*, vol. 29, no. 2, pp. 364–370, Jun. 2006, doi: 10.1109/TCAPT.2006.875874.

[12] S. Gao, J. Hong, J. Kim, S. Choi, and S. Yi, "Effects of Packaging Materials on the Reliability of System in Package," in *2007 8th International Conference on Electronic Packaging Technology*, Shanghai, China, 2007, pp. 1–5, doi: 10.1109/ICEPT.2007.4441427.

[13] V. Carias *et al.*, "Development of Mold Compounds With Ultralow Coefficient of Thermal Expansion and High Glass Transition Temperature for Fan-Out Wafer-Level Packaging," *IEEE Trans. Compon., Packag. Manufact. Technol.*, vol. 5, no. 7, pp. 921–929, Jul. 2015, doi: 10.1109/TCPMT.2015.2443072.

[14] A. Cardoso *et al.*, "Development of Novel High Density System Integration Solutions in FOWLP-Complex and Thin Wafer-Level SiP and Wafer-Level 3D Packages," in *2017 IEEE 67th Electronic Components and Technology Conference (ECTC)*, Orlando, FL, USA, 2017, pp. 14–21, doi: 10.1109/ECTC.2017.163.

[15] J. Radon, "On the determination of functions from their integral values along certain manifolds," *IEEE Trans. Med. Imaging*, vol. 5, no. 4, pp. 170–176, Dec. 1986, doi: 10.1109/TMI.1986.4307775.

[16] E. Topal, L. Markus, and E. Zschech, "Deep learning-based inaccuracy compensation in reconstruction of high resolution XCT data," *Sci Rep*.

[17] E. Topal *et al.*, "Multi–scale X–ray tomography and machine learning algorithms to study MoNi4 electrocatalysts anchored on MoO2 cuboids aligned on Ni foam," *BMC Mat*. 2020

[18] *Avizo*. Thermo Fisher Scientific.

[19] *Simpleware ScanIP*. Synopsys, Inc.

[20] *ANSYS SpaceClaim*. ANSYS, Inc.

[21] *ANSYS*. ANSYS, Inc.

[22] E. Zschech *et al.*, "Laboratory Computed X-Ray Tomography – A Nondestructive Technique for 3D Microstructure Analyis of Materials: The working group 'X-Ray Tomography' is headed by Prof. Dr. Ehrenfried Zschech.," *Practical Metallography*, vol. 55, no. 8, pp. 539–555, Aug. 2018, doi: 10.3139/147.110537.

Emre Topal received the B.S. degree in materials science and engineering from Afyon Kocatepe University, Turkey, in 2013, and the M.S. degree in materials science and engineering from Bursa Technical University, Bursa, Turkey, in 2016. He is currently pursuing the Ph.D. degree in electrical engineering at Dresden University of Technology, Dresden, Germany. From 2017 to 2019, he was a researcher with the Center for Advancing Electronics Dresden and the Dresden Center for Nanoanalysis at Dresden University of Technology. His research interest includes the development of 3D image reconstruction algorithms and image-based numerical

simulations for mechanical characterization of complex material systems.

Ehrenfried Zschech is Department Head for Microelectronic Materials and Nanoanalysis at the Fraunhofer Institute IKTS in Dresden, Germany, which he joined in 2009. His responsibilities include multi-scale materials characterization and reliability engineering. Ehrenfried Zschech received his Dr. rer. nat. degree from Technische Universität Dresden. He managed the Materials Analysis Department at Advanced Micro Devices in Dresden from 1997 to 2009. Ehrenfried Zschech holds an adjunct professorship at Faculty of Chemistry of Warsaw University, Poland, as well as honorary professorships for Nanomaterials at Brandenburg University of Technology Cottbus and for Nanoanalysis at Technische Universität Dresden. Ehrenfried Zschech is Member of the Board of Directors of the Materials Research Society (MRS).

Jürgen Gluch received the diploma degree in material science from TU Dresden, Germany, in 2004. From 2004 to 2007 he was an engineer for an automotive supplier company in Tokyo, Japan. Since 2007 he worked as a Scientist for different research institutes in Dresden. In 2011 he earned his PhD from TU Dresden, Germany. His research interests are focused on high resolution imaging and materials analysis by X-ray and electron microscopy as well as tomography, covering the fields of microelectronic devices and energy storage.

André Clausner finished his Diplomingenieur degree in applied mechanics in 2007 and joined afterwards the International Research Training Group „Materials and Concepts for Advanced Interconnects" working in the field of advanced materials for microelectronics until 2010. He joined Fraunhofer IKTS in 2013 after completing his dissertation at the Technical University Chemnitz in physics, focusing on the area of nanoindentation. The goal of his doctoral work was the evaluation of nanoindentation methods for the determination of yield stresses in various classes of materials. Since 2018 he leads the group Nanomechanics and Reliability for Microelectronics at Fraunhofer IKTS. He brings with him a vast knowledge in the field of (nano/micro-) mechanical behaviour of materials, characterisation methods as well as microelectronics reliability.

André Cardoso, photograph and biography not available at the time of publication.